IEEE Access
Multidisciplinary | Rapid Review | Open Access Journal

Received May 30, 2021, accepted September 6, 2021, date of publication September 10, 2021, date of current version September 24, 2021.

Digital Object Identifier 10.1109/ACCESS.2021.3111619

Improved Back-Stepping Control for Nonlinear Small UAV Systems With Transient Prescribed Performance Design

JIAQI GU, RUISHENG SUN, AND JIEQING CHEN
School of Energy and Power Engineering, Nanjing University of Science and Technology, Nanjing 210000, China
Corresponding author: Ruisheng Sun (rs.sun@njust.edu.cn)

ABSTRACT This paper proposes an improved back-stepping control approach and its application to small nonlinear UAV control systems with uncertainties such as external disturbance. Unlike traditional back-stepping control methods, the idea of prescribed performance function (PPF) is incorporated into the control design, such that both the transient and steady-state control performance can be strictly guaranteed. Moreover, we design a novel tracking differentiator to avoid the ''differential expansion'' problem well caused by the calculation of derivative. Significantly, the function approximators (e.g. neural networks) that are widely used to address the unknown nonlinearities in the nonlinear control designs are not needed. Finally, the numerical simulation verifies the convergence and robustness of the system, and the results show that the control strategy can obtain better transient and steady-state performance.

INDEX TERMS Back-stepping control, nonlinear control, prescribed performance function, robust control, tracking differentiator.

I. INTRODUCTION

At present, UAV technology is occupying an increasingly important position in information-based operations, and it can achieve various combat functions such as cruise detection, precision strike, communication relay, and damage assessment [1]. However, for the small UAV system, it is a complicated nonlinear system with parameter perturbation and external disturbance. In the nonlinear control theory, many various advanced control methods have been explored, such as adaptive control [2]–[4], robust control [5], [6], sliding mode control [7], [8], neural networks control [9], etc.

The UAV with complex shape will cause strong nonlinearity at low speed and large overshoots when maneuvering. Some scholars adopt intelligent control strategy to solve the nonlinearity of UAV system [10]–[13]. However, the above nonlinear control methods do not consider the transient performance under strong nonlinear conditions. For UAV system, if the transient performance cannot be sufficiently constrained, the transient response (such as overshoot, convergence rate, etc.) of the system will be bad before reaching steady state, which will destroy the stability of the system and even cause the failure of the whole system. Therefore, it is of great significance to study the transient performance of UAV control system.

Recently, Bechlioulis and Rovithakis [14], [15] has proposed a prescribed performance control law, which both the transient and steady-state performance can be analytically examined and prescribed. This method introduces a prescribed performance function and a related error transformation. According to this idea, the control performance of the system is greatly improved in engineering applications. Geng *et al.* [16]–[18] carried out prescribed performance controller designs for the extreme value search systems with unknown parameters, control gain and control direction. Sun *et al.* [19] proposed a new design method of non-approximation prescribed performance controller for missile control system. The design process is simple and the control performance is superior. Li *et al.* [20], [21] performed prescribed performance inversion control for non-affine models of hypersonic vehicles and introduced RBF to approximate unknown functions and model uncertainties, which improved the robustness of the control system. Liu [22] developed a trajectory tracking control scheme for a quadrotor unmanned

The associate editor coordinating the review of this manuscript and approving it for publication was Roberto Sacile.

aerial vehicle, and the position constraints and the prescribed performance constraints on attitude tracking errors can be achieved.

On the other hand, the back-stepping control can make full use of the known information of the system to suppress the influence of parameter perturbation and external disturbance. Reference [23] used a combination of back-stepping control and adaptive law to solve the generalized uncertainties existing in the system. However, it is necessary and difficult to calculate the derivative of the virtual control variable for the traditional back-stepping control, which will create ''differential term expansion''. Reference [24] proposed a new tracking differentiator and used it in the robust back-stepping control. Delightedly, the problems caused by derivative calculation have been solved. Madani [25] and Stotsky [26] used sliding mode filters to calculate the virtual control variable derivatives; Yip [27] introduced linear filters to generate differential signals; Farrell [28] proposed a command filter back-steeping design method to effectively avoid cumbersome mathematical calculations. Sharm [29] and Shin [30] treated the derivative of the virtual control variable as an unknown function and used neural networks to approximate it, thereby achieving good results.

Motivated by the above discussions, this article aims to develop an improved back-stepping control strategy for UAV attitude control systems by combining the prescribed performance functions and tracking differentiator techniques. The main contributions can be highlighted as follows.

1) The performance constraints are introduced into the back-stepping control. The global asymptotic stabilization results are obtained of the closed-loop system.
2) A novel tracking differentiator has been developed, which has greatly improved the ability to obtain differential signals. Differential expansion in back-stepping control has been avoided.
3) The achieved tracking control strategy has been utilized to solve the attitude control problems for UAVs.

The structure of this article is as follows. Section II models the nonlinear dynamics of small UAV systems. In Section III, an improved back-stepping control strategy is proposed. Section IV gives the results of numerical simulation verification. Finally, conclusions are drawn in Section V.

II. PROBLEM FORMULATION

In this section, the mathematical model of the UAV system is introduced and the control objectives are briefly described.

A. UAV SYSTEM LONGITUDINAL ATTITUDE DYNAMICS

Figure 1 briefly describes the coordinate system. The center of gravity is selected as the coordinate origin. The Ox axis coincides with the body axis, the head is positive, the Oy axis is pointing up from the body as positive, the Oz axis constitutes a right-handed coordinate system.

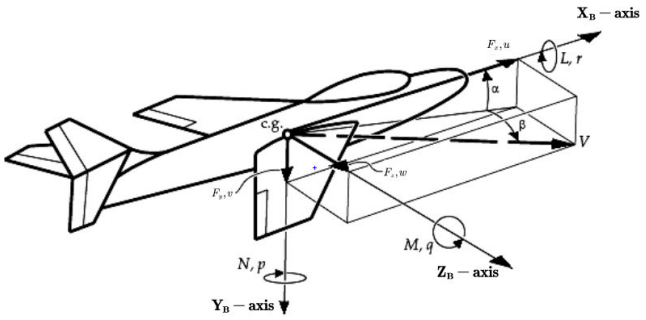

FIGURE 1. Definition of axes, Euler angles, aerodynamic states and moments.

In order to simplify the research, we establish a mathematical model to describe the UAV system in the pitch plane

$$\begin{cases} \dot{\vartheta} = \omega_z \\ \dot{\omega}_z = \dfrac{M_z}{J_z} \end{cases} \tag{2.1}$$

where the states (ϑ, ω_z) are the pitch angle and the pitch angular rate, respectively. J_z is the moment of inertia.

In addition, the pitching moment is a non-linear function of pitch angle, pitch angular rate, and elevator deflection, which is given by

$$\begin{aligned} M_z &= qSLm_z \\ &= qSL\left(m_{z0} + m_z^{\omega_z}\omega_z + m_z^{\alpha}\alpha + m_z^{\delta_e}\delta_e + m_z^{\omega_z^3}\omega_z^3\right) \end{aligned} \tag{2.2}$$

where q, S, L are the dynamic pressure, reference area, reference length, respectively. δ_e is the elevator deflection. The aerodynamic moment coefficient m_{z0} is zero-lift pitching moment coefficient, and else coefficients $m_z^{\omega_z}$, m_z^{α}, $m_z^{\delta_e}$, $m_z^{\omega_z^3}$ are the pitching moment derivatives. The control input is the elevator deflection δ_z.

The uncertainty of the system is caused by unknown external disturbances (such as wind) and the unmodeled dynamics, which can be consider as disturbance terms d_1, d_2. Therefore, the disturbance terms are added to the mathematical model as

$$\begin{cases} \dot{\vartheta} = \omega_z + d_1 \\ \dot{\omega}_z = \dfrac{M_z + \Delta M_z}{J_z} + d_2 \end{cases} \tag{2.3}$$

B. CONTROL MODEL AND OBJECTIVES

For the convenience of controller design, equation (2.3) is rewritten into the general form required for control design, which is given by

$$\begin{cases} \dot{\vartheta} = f_{10}(\vartheta, \omega_z) + f_{1\Delta}(\vartheta, \omega_z) + g_1(\vartheta, \omega_z)\omega_z + d_1 \\ \dot{\omega}_z = f_{20}(\vartheta, \omega_z) + f_{2\Delta}(\vartheta, \omega_z) + g_2(\vartheta, \omega_z)\delta_z + d_2 \\ y = \vartheta \end{cases} \tag{2.4}$$

where f_{10}, f_{20} represent the known dynamics part of the system; $f_{1\Delta}$, $f_{2\Delta}$ represent the unmodeled dynamics of the system, and the combination of unmodeled dynamics and

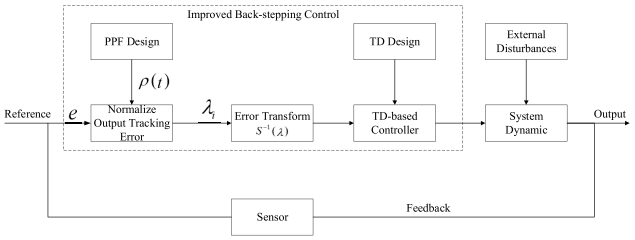

FIGURE 2. Block diagram of the improved back-stepping control.

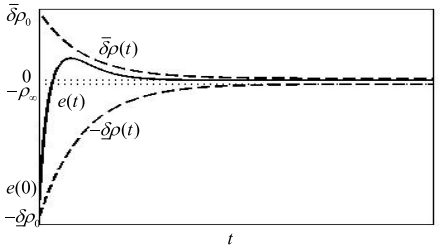

FIGURE 3. Prescribed tracking error bound with $\rho(t)$.

external disturbances are considered as the comprehensive disturbance, denoted as $\xi_i = d_i + f_{i\Delta}(i = 1, 2)$, then the system is rewritten as

$$\begin{cases} \dot{\vartheta} = f_{10}(\vartheta, \omega_z) + g_1(\vartheta, \omega_z)\omega_z + \xi_1 \\ \dot{\omega}_z = f_{20}(\vartheta, \omega_z) + g_2(\vartheta, \omega_z)\delta_e + \xi_2 \\ y = \vartheta \end{cases} \tag{2.5}$$

The following assumption is made for the controller design.

Assumption 1 [31]: The nonlinear functions $F_1 = f_1 + g_1\omega_z + d_1, F_2 = f_2 + g_2\delta_z + d_2$ are continuous, and $\left|\frac{\partial F_1(\vartheta,\omega_z,d_1)}{\partial \omega_z}\right| \geq \varphi_1, \left|\frac{\partial F_2(\vartheta,\omega_z,\delta_z,d_2)}{\partial \delta_z}\right| \geq \varphi_2, \forall(\vartheta, \omega_z, \delta_z) \in \mathbb{R}^3$ are true for positive constants $\varphi_1, \varphi_2 > 0$. Meanwhile, the signs of $\frac{\partial F_1(\vartheta,\omega_z,d_1)}{\partial \omega_z}$ and $\frac{\partial F_2(\vartheta,\omega_z,\delta_e,d_2)}{\partial \delta_z}$ are strictly positive or negative.

This assumption is recognized controllability conditions in nonlinear control designs, and the assumption indicates that the control input gain for all $t > 0$ is non-zero. Without loss of generality, this article assumes that they are all positive.

The main purpose of control design has the following two aspects:

(1) The system output ϑ accurately tracks a given instruction ϑ_c;

(2) The transient and steady state tracking errors $e_1(t) = \vartheta(t) - \vartheta_c(t)$ of the closed-loop system must be within a preset range.

III. IMPROVED BACK-STEPPING CONTROLLER DESIGN

In this section, we will develop an improved back-stepping control design method. PPF and tracking differentiator are introduced into the back-stepping control for improving the control performance. First, we incorporate the prescribed performance function and the transformed errors, and give their definition and concrete expression. Then, a new fast and stable tracking differentiator is developed for the following controller design. Finally, back-stepping control scheme is conducted step by step. The structure of the controller is shown in Figure 2.

A. PRESCRIBED PERFORMANCE FUNCTION AND ERROR TRANSFORMATION

A prescribed performance function (PPF) is introduced to meet transient performance and steady-state performance constraints. The performance function is defined as following:

Definition 1 [12]: Continuous function $\rho(t) : \mathbb{R}_+ \to \mathbb{R}_+$ is the performance function, which satisfies:

(1) $\rho(t)$ is positive and decreasing;

(2) $\lim_{t\to\infty} \rho(t) = \rho_\infty > 0, \lim_{t\to 0} \rho(t) = \rho_0$.

Select the expression of the performance function as

$$\rho(t) = (\rho_0 - \rho_\infty)e^{-lt} + \rho_\infty \tag{3.1}$$

where ρ_0 is the initial error boundary, ρ_∞ is the steady-state error boundary, and l determines the convergence rate. Above three parameters are positive numbers.

Therefore, the control objective (2) can be achieved by making the error $e(t)$ in a set defined in advance with $\rho(t)$ in the form

$$-\underline{\delta}\rho(t) < e_1(t) < \bar{\delta}\rho(t), \quad \forall t > 0 \tag{3.2}$$

where $\underline{\delta}, \bar{\delta}$ are positive constants.

In order to deal with the inequality constraint (3.2), we introduce an error transformation function to convert the inequality constraint into an equality constraint [31]. Here, we define a smooth and strictly increasing function $S(\varepsilon)$ as

$$e(t) = \rho(t)S(\varepsilon) \tag{3.3}$$

where ε is the transformed error. The error transformation function $S(\varepsilon)$ satisfies the following properties:

(1) $-\underline{\delta} < \rho(t)\varepsilon(t) < \bar{\delta}, \forall\varepsilon \in L_\infty$;

(2) $\lim_{\varepsilon\to+\infty} S(\varepsilon) = \bar{\delta}, \lim_{\varepsilon\to-\infty} S(\varepsilon) = -\underline{\delta}$.

Then select the error transformation function as

$$S(\varepsilon) = \frac{\bar{\delta}e^{\varepsilon} - \underline{\delta}e^{-\varepsilon}}{e^{\varepsilon} + e^{-\varepsilon}} \tag{3.4}$$

Because $S(\varepsilon)$ is a smooth and strictly increasing function, the inverse function is

$$\varepsilon(t) = S^{-1}(\lambda) = \frac{1}{2}\ln\left(\frac{\underline{\delta} + \lambda}{\bar{\delta} - \lambda}\right) \tag{3.5}$$

where $\lambda(t) = \frac{e(t)}{\rho(t)}$.

B. TRACKING DIFFERENTIATOR DESIGN

This section designs a novel tracking differentiator based on the sigmoid function to solve the calculation of the derivative of the virtual control variable. First, we need to introduce some theorems about nonlinear tracking differentiator.

Theorem 1 [32]: For the system S

$$S:\begin{cases}\dot{z}_1(t)=z_2(t)\\ \dot{z}_2(t)=f[z_1(t),z_2(t)]\end{cases} \tag{3.6}$$

If its solution $z_1(t)$, $z_2(t)$ satisfies: $\lim_{t\to\infty} z_1(t)=0$, $\lim_{t\to\infty} z_2(t)=0$, then there will be a solution of system S_1 as

$$S_1:\begin{cases}\dot{x}_1(t)=x_2(t)\\ \dot{x}_2(t)=R^2\left\{f\left[x_1(t)-v(t),\dfrac{x_2(t)}{R}\right]\right\}\end{cases} \tag{3.7}$$

For any given integrable function $v(t)$ and constant T, the solution of S_1 satisfies: $\lim_{t\to\infty}\int_0^T |x_1(t)-v(t)|dt=0$ (or $\lim_{t\to\infty}\int_{0+\tau_0}^{T+\tau_0}|x_1(t)-v(t)|dt=0$), $\lim_{t\to\infty} x_2(t)=0$.

Then we use the sigmoid function [24] to design the function expression as

$$h(x)=\frac{1-e^{-\beta x}}{1+e^{-\beta x}} \tag{3.8}$$

where β is a positive constant to adjust the width of the approximate linear region of the function.

Remark 1: The function $h(x)$ has the following characteristics:

(1) When the independent variable approaches 0, it shows a good linear characteristic; when the independent variable takes a large value, it shows a saturated characteristic; and the function is globally smooth.

(2) Thus, this function can not only speed up its global convergence, but also make the tracking response smoother, and avoid high-frequency vibration.

According to the above analysis, the specific form of the construction system S_2 is as follows:

$$\begin{cases}\dot{x}_1(t)=x_2(t)\\ \dot{x}_2(t)=-ah(x_1)-bh(x_2)-ch^n(x_2)\end{cases} \tag{3.9}$$

The stability conclusion of the tracking differentiator proposed in this paper is as follows:

Theorem 2: For the system S_2, when $a>0$, $b>0$, $c>0$, and the positive parameter n is odd. The solution of the equation (3.5) satisfies the Theorem 1.Therefore the system S_2 is gradually stable, and converges to $(x_1,x_2)^T=(0,0)^T$, which means $\lim_{t\to\infty} x_1(t)=0$, $\lim_{t\to\infty} x_2(t)=0$. The proof of stability is as follows:

Proof: Select Lyapunov function

$$V=\int_0^{x_1} ah(\tau)\,d\tau+\frac{1}{2}x_2^2 \tag{3.10}$$

$h(x)$ is an odd function, $xh(x)>0$, according to the nature of the definite integral, we get $\int_0^{x_1} ah(\tau)\,d\tau>0$, so $V>0$. When $x_1\to\infty, x_2\to\infty$, $\int_0^{x_1} ah(\tau)\,d\tau\to\infty$, $\frac{1}{2}x_2^2\to\infty$ is true. Therefore, when $\begin{bmatrix}x_1 & x_2\end{bmatrix}\to\infty$, $V(x_1,x_2)\to\infty$ holds.

Differentiate $V(x_1,x_2)$ with time to as

$$\dot{V}=\dot{x}_1 ah(x_1)+\dot{x}_2 x_2 \tag{3.11}$$

According to (3.5)

$$\begin{aligned}\dot{V}&=ax_2h(x_1)+x_2\left(-ah(x_1)-bh(x_2)-ch^n(x_2)\right)\\&=-bx_2h(x_2)-cx_2h^n(x_2)\end{aligned} \tag{3.12}$$

where $x_2h(x_2)>0$ holds for $x_2\neq 0$, and n is odd, thus $x_2h^n(x_2)>0$, so we can get

$$\dot{V}(x_1,x_2)<0 \tag{3.13}$$

$\dot{V}(x_1,x_2)=0$ holds if and only if $x_2=0$.

When $x_1\neq 0$, there is $\dot{x}_2\neq 0$, that is, x_2 is unstable at 0, indicating that there is no point outside the origin that satisfies $\dot{V}(x_1,x_2)=0$. Therefore, the solution of the system S_2 is globally asymptotically stable.

Design the tracking differentiator based on Theorem 1 as

$$\begin{cases}\dot{x}_1(t)=x_2(t)\\ \dot{x}_2(t)=R^2\{-ah[x_1(t)-v(t)]\\ \quad -bh\left[\dfrac{x_2(t)}{R}\right]-ch^n\left[\dfrac{x_2(t)}{R}\right]\end{cases}\Bigg\} \tag{3.14}$$

where $a>0, b>0, c>0, n>0$ are positive and odd design parameters, and $v(t)$ is the signal to be tracked.

According to Theorem 1 and the above analyses, for any bounded integrable function $v(t)$ and any positive number$T$, the solution of formula (3.10) can satisfy $\lim_{t\to\infty}\int_0^T |x_1(t)-v(t)|dt=0$. The designed tracking differentiator can theoretically track and differentiate the input signal.

C. CONTROL DESIGN

In this section, an improved back-stepping controller is developed based on PPF and TD. The design process is divided into the following two steps:

Step 1: Define tracking error as $e_1=\vartheta-\vartheta_c$, PPF $\rho_1=(\rho_{10}-\rho_{1\infty})e^{-l_1 t}+\rho_{1\infty}$. According to the equation (3.5), transformed error is given as

$$\varepsilon_1(t)=S^{-1}(\lambda_1)=\frac{1}{2}\ln\left(\frac{\delta_1+\lambda_1}{\delta_1-\lambda_1}\right) \tag{3.15}$$

where $\lambda_1=e_1/\rho_1$.

Derivative of ε_1 is

$$\begin{aligned}\dot{\varepsilon}_1&=\frac{\partial S^{-1}}{\partial\left(\frac{e_1}{\rho_1}\right)}\frac{1}{\rho_1}\left(f_{10}+g_1\omega_z+\xi_1-\dot{\vartheta}_c-\nu_1\right)\\&\triangleq r_1\left(f_{10}+g_1\omega_z+\xi_1-\dot{\vartheta}_c-\nu_1\right)\end{aligned} \tag{3.16}$$

where $r_1=\frac{\partial S^{-1}}{\partial\left(\frac{e_1}{\rho_1}\right)}\frac{1}{\rho_1}$, $\nu_1=\frac{e_1\dot{\rho}_1}{\rho_1}$.

Then we define $\hat{\xi}_1$ as the estimated value of comprehensive disturbance ξ_1, so the estimation error is written as $\tilde{\xi}_1=\xi_1-\hat{\xi}_1$. Select Lyapunov function

$$V_1=\frac{1}{2}\varepsilon_1^T r_1^{-1}\varepsilon_1+\frac{1}{2}\tilde{\xi}_1^T Q_1\tilde{\xi}_1 \tag{3.17}$$

Derivative of V_1

$$\dot{V}_1=\varepsilon_1^T r_1^{-1}\dot{\varepsilon}_1-\tilde{\xi}_1^T Q_1\dot{\hat{\xi}}_1$$

$$= \varepsilon_1^T \left(f_{10} + g_1\omega_z + \xi_1 - \dot{\vartheta}_c - v_1\right) - \tilde{\xi}_1^T Q_1 \dot{\hat{\xi}}_1 \quad (3.18)$$

where Q_1 is a positive definite matrix.

Design the virtual control quantity ω_{zd} as

$$\omega_{zd} = -g_1^{-1}\left(f_{10} + \hat{\xi}_1 - \dot{\vartheta}_c - v_1 + k_1\varepsilon_1\right) \quad (3.19)$$

where the gain k_1 is the positive parameter to be designed.

The estimation law of comprehensive disturbance ξ_1 is

$$\dot{\hat{\xi}}_1 = Q_1^{-1}\varepsilon_1 \quad (3.20)$$

Substituting (3.20) and (3.21) into (3.19)

$$\begin{aligned}\dot{V}_1 &= \varepsilon_1^T r_1^{-1}\dot{\varepsilon}_1 - \tilde{\xi}_1^T Q_1 \dot{\hat{\xi}}_1 \\ &= \varepsilon_1^T \left(f_{10} + g_1\omega_z + \xi_1 - \dot{\vartheta}_c - v_1\right) - \tilde{\xi}_1^T Q_1 \dot{\hat{\xi}}_1 \\ &= -k_1\varepsilon_1^T\varepsilon_1 \le 0 \end{aligned} \quad (3.21)$$

which shows that the variable ε_1 will converge with the action of the virtual controller.

Step 2: The tracking error of the intermediate state quantity ω_z is defined as $e_2 = \omega_z - \omega_{zd}$, and ω_{zd} is the virtual control quantity. Meanwhile, the prescribed performance function is $\rho_2 = (\rho_{20} - \rho_{2\infty})\, e^{-l_2 t} + \rho_{2\infty}$. According to the equation (3.15)

$$\varepsilon_2(t) = S^{-1}(\lambda_2) = \frac{1}{2}\ln\left(\frac{\delta_2 + \lambda_2}{\delta_2 - \lambda_2}\right) \quad (3.22)$$

where $\lambda_2 = e_2 / \rho_2$.

Derivative of ε_2

$$\begin{aligned}\dot{\varepsilon}_2 = &\frac{\partial S^{-1}}{\partial\left(\frac{e_2}{\rho_2}\right)}\frac{1}{\rho_2}\left(f_{20} + g_2\delta_z + \xi_2 - \dot{\omega}_{zd} - v_2\right) \\ &r_2\left(f_{20} + g_2\delta_z + \xi_2 - \dot{\omega}_{zd} - v_2\right)\end{aligned} \quad (3.23)$$

where $r_2 = \frac{\partial S^{-1}}{\partial\left(\frac{e_2}{\rho_2}\right)}\frac{1}{\rho_2}$, $v_2 = \frac{e_2\dot{\rho}_2}{\rho_2}$.

As in step 1, $\hat{\xi}_2$ is defined as the estimated value of the integrated disturbance ξ_2, and $\tilde{\xi}_2 = \xi_2 - \hat{\xi}_2$ is the estimated error. Select Lyapunov function

$$V_2 = V_1 + \frac{1}{2}\varepsilon_2^T r_2^{-1}\varepsilon_2 + \frac{1}{2}\tilde{\xi}_2^T Q_2 \tilde{\xi}_2 \quad (3.24)$$

Derivative of V_2

$$\begin{aligned}\dot{V}_2 &= \dot{V}_1 + \varepsilon_2^T r_2^{-1}\dot{\varepsilon}_2 - \tilde{\xi}_2^T Q_2 \dot{\hat{\xi}}_2 \\ &= \dot{V}_1 + \varepsilon_2^T\left(f_{20} + g_2\delta_z + \xi_2 - \dot{\omega}_{zd} - v_2\right) - \tilde{\xi}_2^T Q_2 \dot{\hat{\xi}}_2\end{aligned} \quad (3.25)$$

where Q_2 is a positive definite matrix.

It is easily seen that $\dot{\omega}_{zd}$ appears in $\dot{V}_2$, so the tracking differentiator designed is introduced in Part III to deal with this item. The tracking differentiator is designed as follows:

$$\begin{cases}\dot{q}_d = v \\ \dot{v} = R^2\left\{-ah\left[\beta\left(q_d - \omega_{zd}\right)\right] - bh\left[\frac{v}{R}\right] - ch^n\left[\frac{v}{R}\right]\right\}\end{cases} \quad (3.26)$$

where a, b, c, β, n are the tracker parameters to be designed. q_d is the virtual control derivative.

Finally, the control law is designed as

$$\delta_z = -g_2^{-1}\left(f_{20} + \hat{\xi}_2 - v_2 - \dot{\omega}_{zd} + k_2\varepsilon_2\right) \quad (3.27)$$

where the gain k_2 is a positive parameter.

The estimation law for comprehensive disturbance ξ_2 is

$$\dot{\hat{\xi}}_2 = Q_2^{-1}\varepsilon_2 \quad (3.28)$$

Substituting (3.28) and (3.29) into (3.26)

$$\begin{aligned}\dot{V}_2 &= \dot{V}_1 + \varepsilon_2^T r_2^{-1}\dot{\varepsilon}_2 - \tilde{\xi}_2^T Q_2 \dot{\hat{\xi}}_2 \\ &= \dot{V}_1 + \varepsilon_2^T\left(f_{20} + g_2\delta_z + \xi_2 - \dot{\omega}_{zd} - v_2\right) - \tilde{\xi}_2^T Q_2 \dot{\hat{\xi}}_2 \\ &= -k_1\varepsilon_1^T\varepsilon_1 - k_2\varepsilon_2^T\varepsilon_2 \le 0\end{aligned} \quad (3.29)$$

According to the Lyapunov stability theory, the closed-loop system is gradually stable.

From the above design process, the design method can guarantee the transient and steady-state performance for small UAV system. In addition, the proposed tracking differentiator can solve the ''differential expansion'' problem caused by the calculation of derivative well.

IV. NUMERICAL SIMULATION

Case 1: Research on Tracking Differentiator Simulation

In order to study the tracking characteristics of the proposed tracking differentiator further, a comparative numerical simulation with the tangent sigmoid tracking differentiator (TSTD) in [24], second-order nonlinear tracking differentiator (SNTD) in [32] and arbitrary-order exact robust differentiator (AERD) in [33] is conducted to verify the proposed tracker has fast convergence speed and tracking accuracy. Here step signal and unit sinusoidal signal are both selected as input signals. The design parameters of the tracking differentiator in this paper are set as: $R = 3$, $\beta = 5$, $h_1 = 40$, $h_2 = 20$, $h_3 = 20$, $n = 3$, and the simulation step is 0.001s. The parameters of the other three kinds of tracking differentiators are set according to the corresponding literature [24], [32], [33].

Figure 4 provides the comparative simulation results of the four tracking differentiators. From Figure 4(a) and (b), the proposed TD in this paper can accurately track step signal, while both the transient and steady-state performance can be guarantee. However, the TSTD leads to an aggressive transient response with fairly large overshoot although it can converge. On the other hand, it is also found that the SNTD takes a long time to achieve convergence, where exists a large overshoot. Moreover, the AERD leads to a significant tracking error. Figure 4(c) shows the result of calculating step signal differentiation. One may find that the differential result of the proposed TD satisfies the situation, but the rate of change is very large when the signal produces a step change. Nevertheless, large overshoot occurs when the TSTD calculates the differential of step signal. However, the SNTD takes a long time to converge and has a low intensity of impulse signal. The AERD has a weak ability to obtain the differential signal although the convergence rate is faster than other three tracking differentiators.

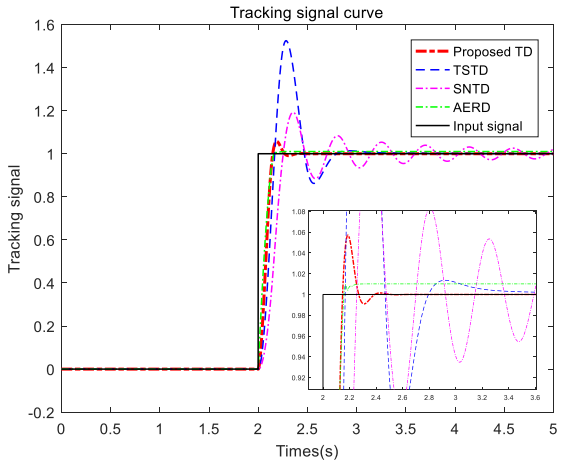

(a). Tracking signal curve

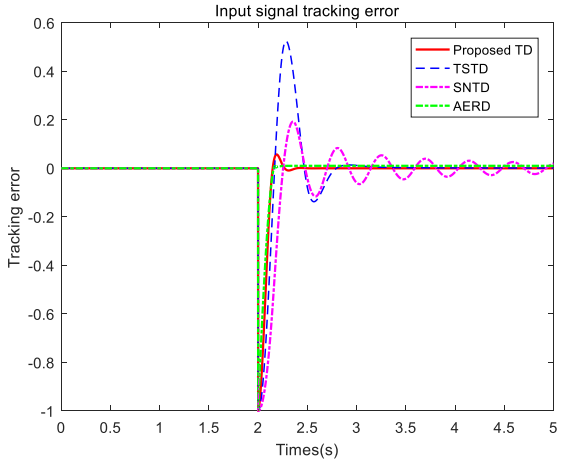

(b). Input signal tracking error

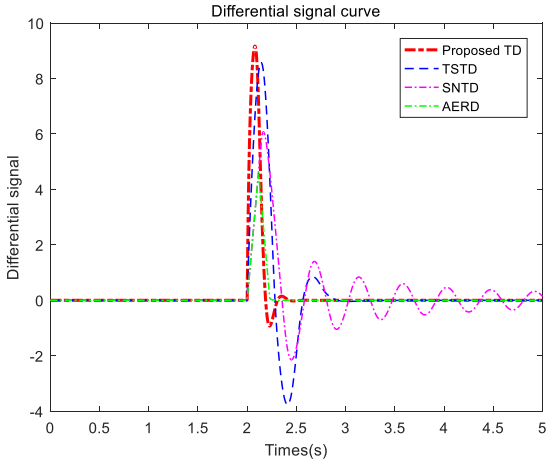

(c).Differential signal

FIGURE 4. Research on tracking differentiator performance.

Next, we investigate the tracking of sinusoidal signals and the extraction of differential signals. The parameters of the tracking differentiator in this paper are set as: $R = 15$, $\beta = 20$, $h_1 = 10$, $h_2 = 10$, $h_3 = 10$, $n = 3$.

TABLE 1. System parameter nominal value.

Symbol	Parameters	Value
J_z	Pitch inertia	0.6451965
M_{z0}	Pitch moment coefficient at $\alpha = \delta_z = \omega_z = 0$	-10.42316
$M_z^{\omega_z}$	Pitch moment derivatives for ω_z	-0.65739
M_z^{α}	Pitch moment derivatives for α	-38.81179
$M_z^{\delta_z}$	Pitch moment derivatives for δ_z	-98.17103
$M_z^{\omega_z^3}$	Pitch moment derivatives for ω_z^3	-51.61572

The simulation results are shown in Figure 5. From Figure 5 (a) and (b), we can see that the TD proposed in this paper and the AERD achieve fast tracking of sinusoidal signal, with small tracking error and no vibration. However, the TSTD has high-frequency vibration and slow convergence rate. Obviously, the SNTD has a large tracking error and cannot accurately track the input signal. As seen from Figure 5 (c) and (d), the proposed TD can solve the differential signal of the input signal with higher accuracy, and can quickly converge. But it takes a long time for TSTD to obtain an accurate differential signal, and it has a large vibration in the initial stage. Similarly, there is a large tracking error when SNTD extracts the differential signal, and it cannot converge to a small set for a long time. Moreover, when AERD calculates differential signal, the vibration occurs in the part with larger curvature, and the calculated differential curve is not smooth. By comparing the tracking characteristics of different tracking differentiators, the proposed TD improves the convergence rate and reduces high-frequency vibration. It can track the input signal quickly and stably, and can obtain accurate and smooth differential signals.

Case 2: Control Simulation

In order to verify the effectiveness of the improved back-stepping control method proposed in this paper (prescribed performance back-stepping control, PPBC), this section compares with traditional back-stepping control (BSC) and feedback linearization control (FLC). We mainly study the control performance of control system, especially the transient performance (such as overshoot, convergence rate, etc.). The initial state of the system is $\vartheta_0 = 0$ and $\omega_0 = 0$, and the simulation step is taken as 0.01s. The control command is $\vartheta_c = 1$ deg and $\vartheta_c = \cos(t)$ deg, the relevant parameters are listed in Table 1.

The controller parameters designed in this paper are as follows:

$$\rho_1 = (1.2 - 0.01)\, e^{-15t} + 0.01 \rho_2 = (16 - 0.4)\, e^{-15t} + 0.4$$
$$\underline{\delta} = \overline{\delta} = 1, \quad k_1 = 0.03,\ k_2 = 20,\ Q_1 = 10,\ Q_2 = 10.$$

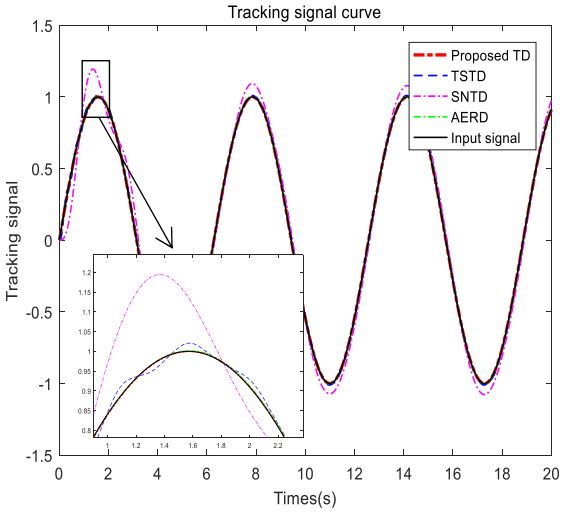

(a). Tracking signal curve

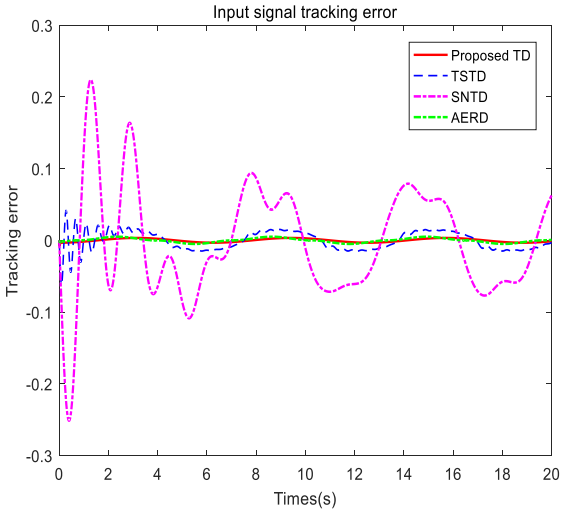

(b). Input signal tracking error

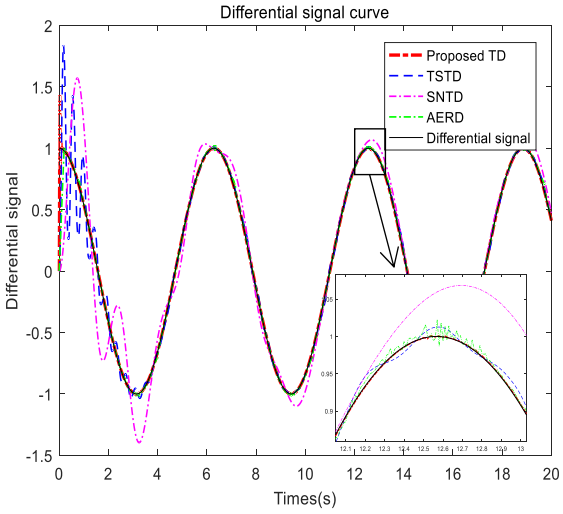

(c).Differential signal

FIGURE 5. Research on tracking differentiator performance.

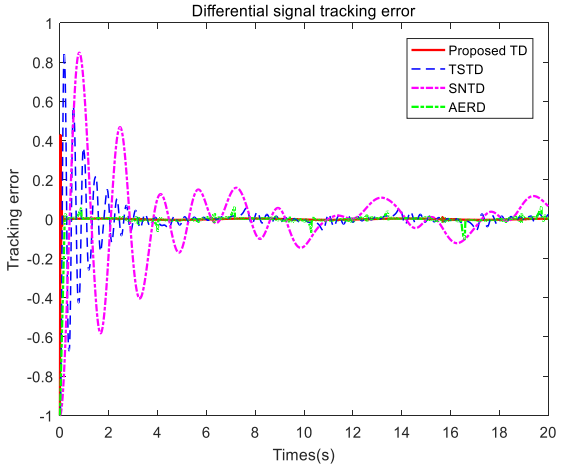

(d).Differential signal tracking error

FIGURE 5. *(Continued.)* Research on tracking differentiator performance.

The traditional back-stepping controller (BSC) is designed as follows:

$$e_1 = \vartheta - \vartheta_c, \quad q_d = -\left(\hat{d}_1 + k_1 e_1\right)$$
$$e_2 = \omega_z - q_d, \quad \delta_z = -g_x^{-1}\left(f_{20} + \hat{d}_2 - \dot{q}_d + k_2 e_2\right)$$
$$\hat{d}_1 = e_1/Q_1, \hat{d}_2 = e_2/Q_2$$
$$k_1 = 20, \quad k_2 = 20, \; Q_1 = Q_2 = 0.01.$$

The feedback linearization controller (FLC) is designed as follows [34]:

$$e_1 = \vartheta - \vartheta_c, e_2 = \omega_z - \dot{\vartheta}_c$$
$$s = -[k_1, k_2][e_1, e_2]^T$$
$$\delta_z = -\frac{K}{g_2}(\dot{\omega}_z - s), \quad K = 6, \; k_1 = 20, \; k_2 = 5$$

A. CONTROL SIMULATION OF NONLINEAR UAV SYSTEM

Figure 6 shows the comparative numerical simulation results of three control methods: PPBC, BSC, and FLC. All three methods track control commands accurately, but their tracking performances are different. Figures 6 (b) and (d) show that PPBC's pitch angle tracking error and pitch angular rate tracking error can be limited to prescribed boundaries, but the tracking errors of the other two methods are beyond the boundaries. At the same time, there is a significant difference in the tracking of pitch angular rate, BSC and FLC have large overshoots and the convergence time of them needs about 0.35s, while PPBC only needs less than 0.1s and without overshoot. Compared with the other two methods, PPBC has better transient performance. Through this example, we verify the effectiveness of PPBC and its advantages in transient performance.

B. CONTROL SYSTEM ROBUSTNESS ANALYSIS

In order to further study the robustness of the control system designed, the system external disturbance is considered. The

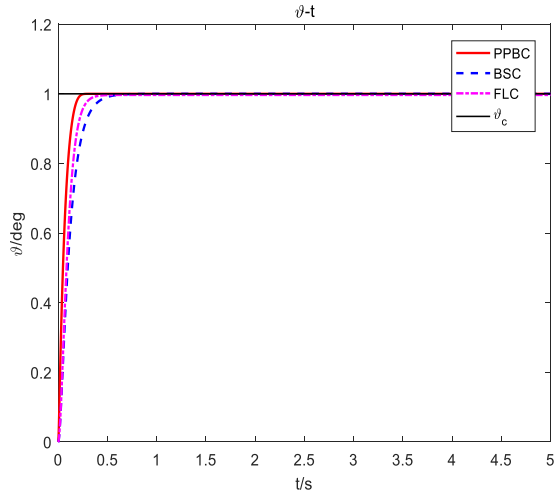

(a). Response of pitch angle ϑ

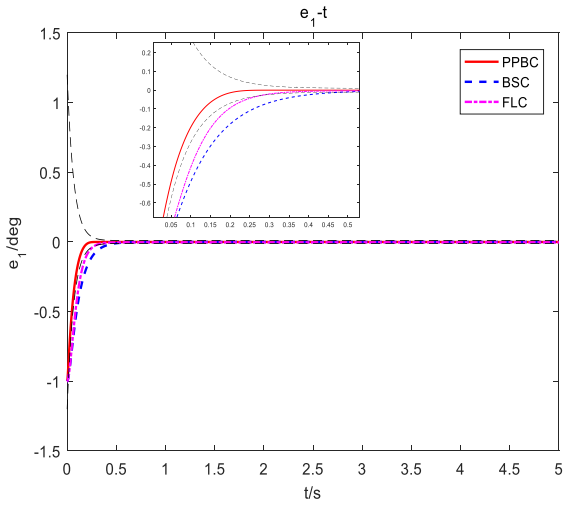

(b). Tracking errors of ϑ

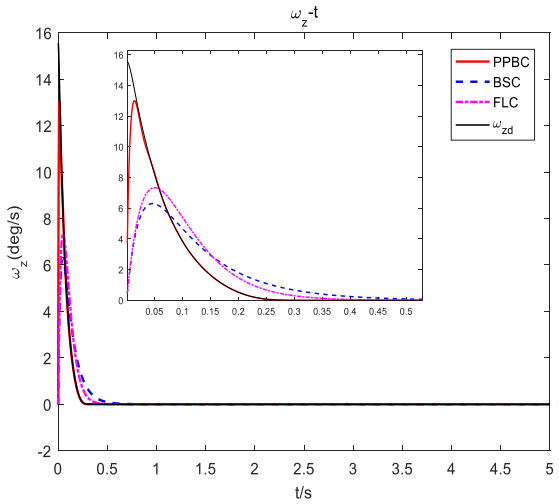

(c). Response of pitch angular rate ω_z

FIGURE 6. Numerical simulation results.

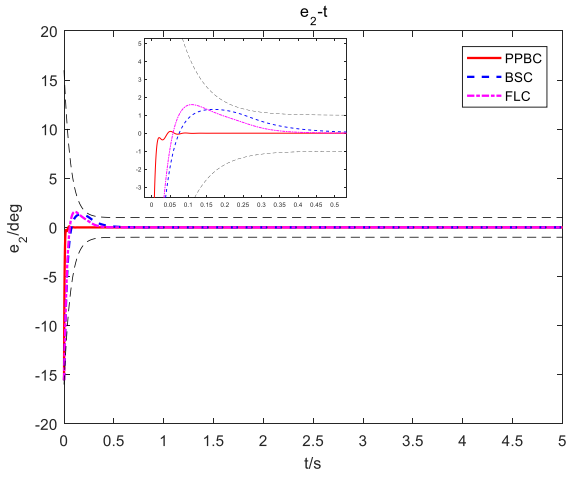

(d). Tracking errors of ω_z

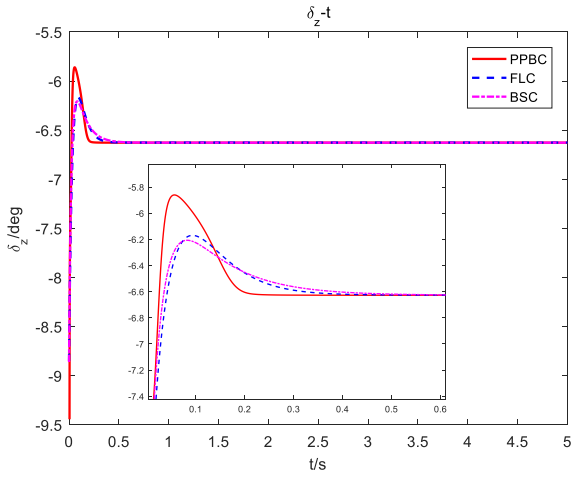

(e). Control signals

FIGURE 6. ***(Continued.)*** **Numerical simulation results.**

other conditions are the same with those in Case A. The comprehensive disturbance is selected as $\xi_1 = \xi_2 = 5\sin(2\pi t)$.

The simulation results are shown in Figure 7. According to Figure 7 (a) and (c), in the case of external disturbances in the system, PPBC can successfully compensate for the impact of disturbances and accurately track input command. The BSC can also converge to the input command over time, while FLC has a large error and cannot track the command accurately. As shown in Figure 7 (b) and (d), the error curves of PPBC can be limited to prescribed boundaries, it convergences quickly, and the steady-state error is small and without vibration. Although BSC can converge eventually, it has a large overshoot in the convergence process and a slow convergence rate. Moreover, the errors still vibrate slightly during a long time. Therefore, the steady-state and transient performance of BSC is inferior to that of PPBC. For FLC, it is difficult to compensate the unknown disturbances, so it has obvious tracking errors, and the control performances are

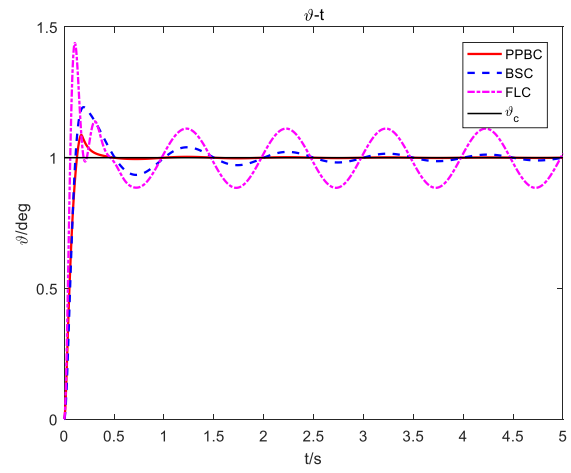

(a). Response of pitch angle ϑ

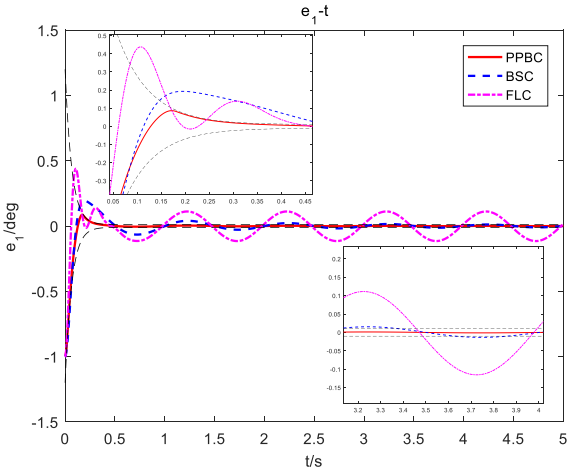

(b). Tracking errors of ϑ

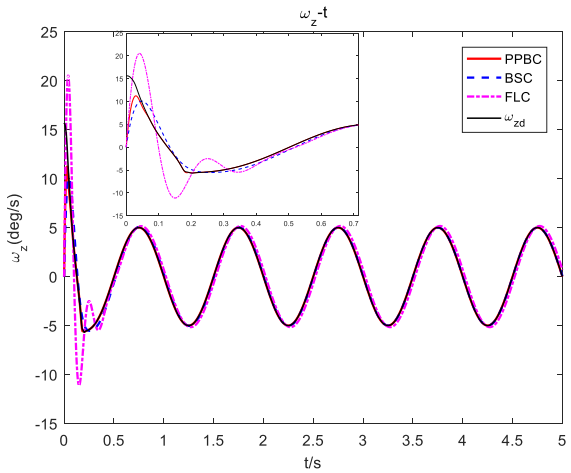

(c). Response of pitch angular rate ω_z

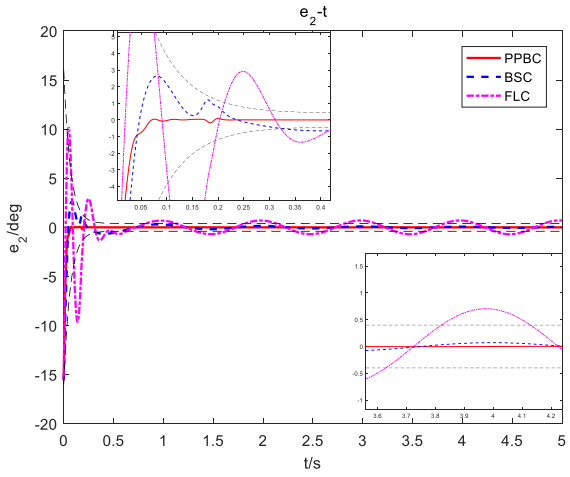

(d). Tracking errors of ω_z

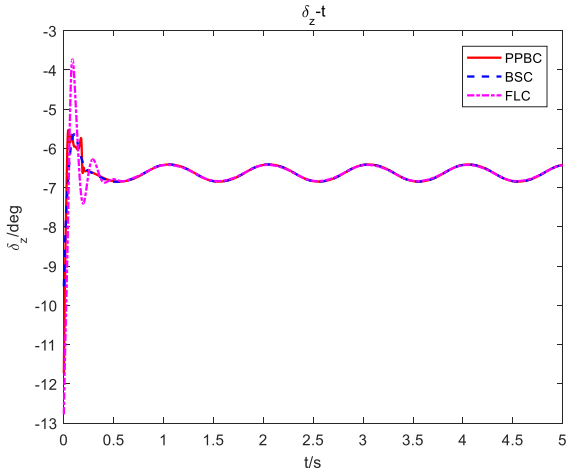

(e). Control signals

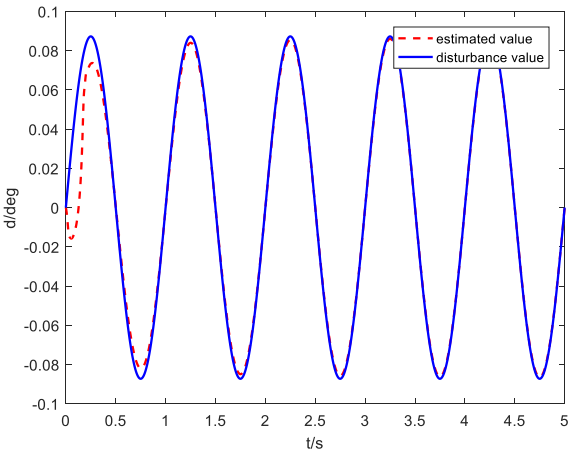

(f). Adaptive estimation law

FIGURE 7. Numerical simulation results $\vartheta_c = 1$ deg.

not as good as the other two methods. Figure (e) shows that the control signals are stable and there is no high-frequency vibration. From the figure (f) we can see that the designed estimate law can estimate the disturbance term accurately. Through the above analysis, we can conclude that PPBC can successfully compensate the influence of the disturbances

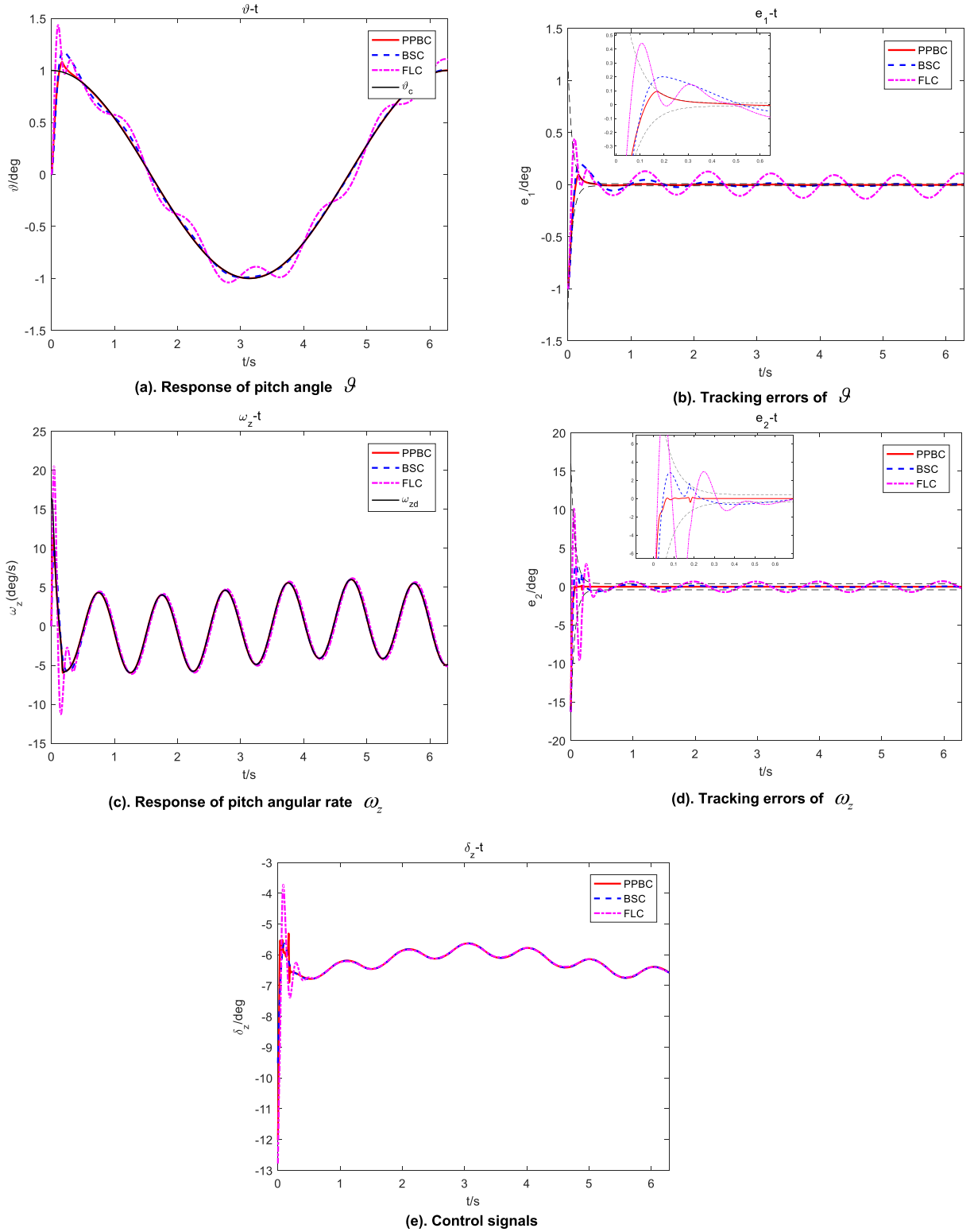

FIGURE 8. Numerical simulation results ϑ_c=cos (t) deg.

in the presence of external disturbances. Meanwhile, both transient and steady state performance meet the requirements of the performance function.

C. TRAJECTORY SIMULATION

In the above simulation, the control command ϑ_c is the unit step signal, which verifies the effectiveness of the proposed

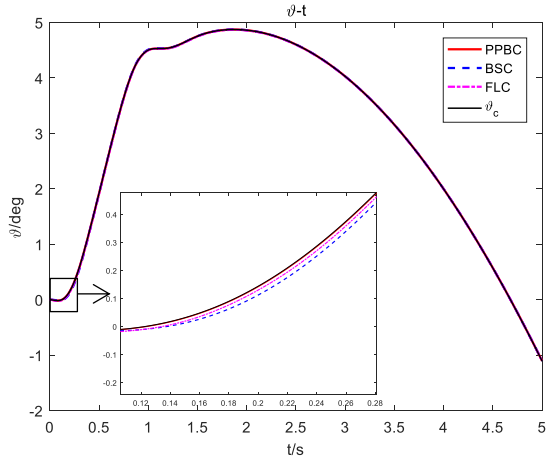

(a). Response of pitch angle ϑ

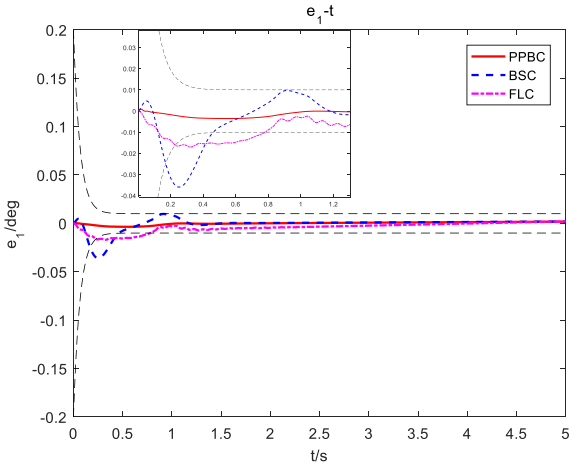

(b). Tracking errors of ϑ

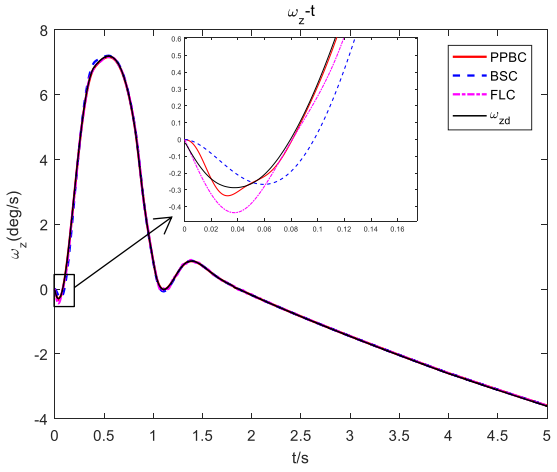

(c). Response of pitch angular rate ω_z

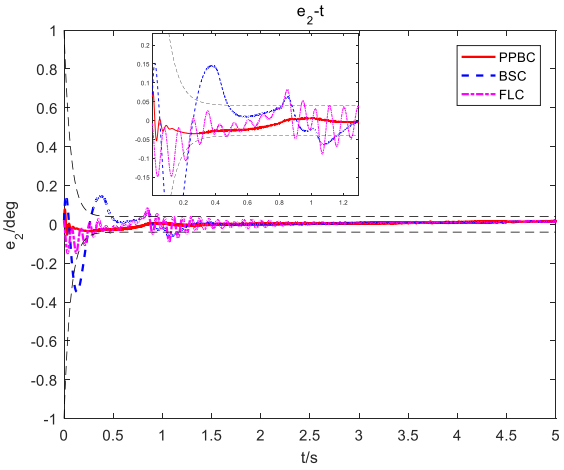

(d). Tracking errors of ω_z

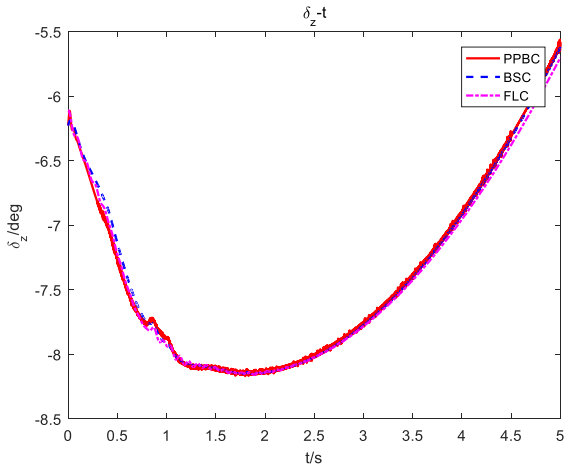

(e) Control signal

FIGURE 9. Numerical simulation results.

PPBC. In this case, in order to study the practical engineering application ability of the controller, we take the command of a certain trajectory as the control command and observe the response of the system.

Figure 9 shows the numerical simulation comparison results of the three control methods when the control command is an actual trajectory command. As shown in the figure (a) and (c) that these three control methods can track the command accurately. Since the back-stepping control can use more system information, such as the derivative information of the control command, the control performance can be improved under the condition of making full use of the known information of the system. PPBC combines back-stepping control and PPF, which can limit the range of tracking error by setting the boundary functions, so that the tracking errors are always within a small range, thus ensuring good transient and steady-state performance. FLC method uses less system information than the other two methods, and its control performances are far worse than PPBC and BSC.

It can be seen from Figure 9 (b) and (d) that the error curves of FLC exceed the prescribed boundaries, and they are accompanied by some vibration, especially the tracking error of ω_z, which has large vibration and takes a long time to reach steady state. And the error curves of BSC have a large overshoot, and the convergence rate is slow. Compared with the other two methods, PPBC improves the transient performance, the tracking errors have a fast convergence rate and a small overshoot, and the convergence process is stable without vibration.

V. CONCLUSION

This paper proposes an improved back-stepping control method for nonlinear UAV systems with uncertainties and external disturbances. By introducing a prescribed performance function and error transformation function, the controller can design the transient and steady-state performance of the system quantitatively. Meanwhile, a novel tracking differentiator designed in this paper is introduced into the control design to solve the ''differential expansion'' problem in traditional back-stepping control. The cost of this method is small and no complex neural network approximator is needed, so the development of the controller is not complicated. The proposed systematic recursive control design procedure can also be extended to high-order systems.

Numerical simulation results verify the effectiveness of the method and it can be seen from the simulation results that, whether it is a step signal command or a real signal command, the control method proposed in this paper can complete the control task well, and has greatly improved the control performance and the robustness of the system. The proposed method relies on the complete information. In the subsequent work, the control method will continue to be improved to make it independent of the complete information of the system.

REFERENCES

[1] Y. C. Y. Song and Q. Jiang, ''Development trend and performance analysis of foreign typical cruise missiles,'' *Aircr. Missiles*, vol. 2, no. 2, pp. 37–40, 2013.

[2] A. Teel, R. Kadiyala, P. Kokotovic, and S. Sastry, ''Indirect techniques for adaptive input-output linearization of non-linear systems,'' *Int. J. Control*, vol. 53, no. 1, pp. 193–222, Jan. 1991.

[3] D. G. Taylor, P. V. Kokotovic, R. Marino, and I. Kannellakopoulos, ''Adaptive regulation of nonlinear systems with unmodeled dynamics,'' *IEEE Trans. Autom. Control*, vol. 34, no. 4, pp. 405–412, Apr. 1989.

[4] S. S. Sastry and A. Isidori, ''Adaptive control of linearizable systems,'' *IEEE Trans. Autom. Control*, vol. 34, no. 11, pp. 1123–1131, Nov. 1989.

[5] Y. Hashimoto, ''Robust output tracking of nonlinear systems with mismatched uncertainties,'' *Int. J. Control*, vol. 72, no. 5, pp. 411–417, Jan. 1999.

[6] Z. Qu and Y. Jin, ''Robust control of nonlinear systems in the presence of unknown exogenous dynamics,'' *IEEE Trans. Autom. Control*, vol. 48, no. 2, pp. 336–343, Feb. 2003.

[7] Y.-J. Huang, T.-C. Kuo, and S.-H. Chang, ''Adaptive sliding-mode control for nonlinearsystems with uncertain parameters,'' *IEEE Trans. Syst., Man, Cybern. B. Cybern.*, vol. 38, no. 2, pp. 534–539, Apr. 2008.

[8] T. Shima, M. Idan, and O. M. Golan, ''Sliding-mode control for integrated missile autopilot guidance,'' *J. Guid., Control, Dyn.*, vol. 29, no. 2, pp. 250–260, 2006.

[9] K. S. Narendra and K. Parthasarathy, ''Identification and control of dynamical systems using neural networks,'' *IEEE Trans. Neural Netw.*, vol. 1, no. 1, pp. 4–27, Mar. 1990.

[10] Y. Wang, X. Yang, and H. Yan, ''Reliable fuzzy tracking control of near-space hypersonic vehicle using aperiodic measurement information,'' *IEEE Trans. Ind. Electron.*, vol. 66, no. 12, pp. 9439–9447, Dec. 2019.

[11] Y. Wang, W. Zhou, J. Luo, H. Yan, H. Pu, and Y. Peng, ''Reliable intelligent path following control for a robotic airship against sensor faults,'' *IEEE/ASME Trans. Mechatronics*, vol. 24, no. 6, pp. 2572–2582, Dec. 2019.

[12] M. Rabah, A. Rohan, S. A. S. Mohamed, and S.-H. Kim, ''Autonomous moving target-tracking for a UAV quadcopter based on fuzzy-PI,'' *IEEE Access*, vol. 7, pp. 38407–38419, 2019.

[13] N. Fethalla, M. Saad, H. Michalska, and J. Ghommam, ''Robust observer-based dynamic sliding mode controller for a quadrotor UAV,'' *IEEE Access*, vol. 6, pp. 45846–45859, 2018.

[14] C. P. Bechlioulis and G. A. Rovithakis, ''Approximation-free prescribed performance control for unknown SISO pure feedback systems,'' in *Proc. Eur. Control Conf. (ECC)*, Jul. 2013, pp. 4544–4549.

[15] C. P. Bechlioulis and G. A. Rovithakis, ''Robust adaptive control of feedback linearizable MIMO nonlinear systems with prescribed performance,'' *IEEE Trans. Autom. Control*, vol. 53, no. 9, pp. 2090–2099, Oct. 2008.

[16] Y. A. Hu, B. L. Geng, and Y. T. Zhao, ''Prescribed performance backstepping control of strict feedback nonlinear systems,'' *Control Decis.*, vol. 29, no. 8, pp. 1509–1512, 2014.

[17] B. L. Geng, Y. A. Hu, J. Li, and Y. T. Zhao, ''Prescribed performance backstepping control of uncertain systems with unknown control gains,'' *Zidonghua Xuebao/Acta Automatica Sinica*, vol. 40, no. 11, pp. 2521–2529, 2014.

[18] B. L. Geng and Y. A. Hu, ''Prescribed performance adaptive neural backstepping control for nonlinear system with uncertainties and unknown control directions,'' *Control Theory Appl.*, vol. 31, no. 3, pp. 397–403, 2014.

[19] R. Sun, J. Na, and B. Zhu, ''Robust approximation-free prescribed performance control for nonlinear systems and its application,'' *Int. J. Syst. Sci.*, vol. 49, no. 3, pp. 511–522, Feb. 2018.

[20] X. LI, S. Zhao, and X. Bu, ''Design of prescribed performance backstepping control method for hypersonic flight vehicles,'' *J. Beijing Univ. Aeronaut. Astronaut.*, vol. 45, no. 4, pp. 650–661, 2019.

[21] X. Li, S. Zhao, and X. Bu, ''Prescribed performance control method for non-affine model of hypersonic vehicles,'' *Control Theory Appl.*, vol. 36, no. 5, pp. 1672–1681, 2019.

[22] Z. Liu, L. Xiong, and W. Shi, ''Trajectory tracking control for a QUAV with performance constraints,'' *IEEE Access*, vol. 7, pp. 142467–142477, 2019.

[23] Y. A. Hu, J. Y. Q., and Z. X., ''Robust adaptive design of BTT missile block model,'' *J. Astronaut.*, vol. 25, no. 3, pp. 225–230, 2004.

[24] T. Shi-Li, L. Hu-Min, and W. Peng-Fei, ''Backstepping control for hypersonic vehicle with a novel tracking differentiator,'' *J. Astronaut.*, no. 6, pp. 673–683, 2019.

[25] T. Madani and A. Benallegue, ''Control of a quadrotor mini-helicopter via full state backstepping technique,'' in *Proc. 45th IEEE Conf. Decis. Control*, Dec. 2006, pp. 1515–1520.

[26] A. Stotsky, J. K. Hedrick, and P. P. Yip, ''The use of sliding modes to simplify the backstepping control method,'' in *Proc. Amer. Control Conf.*, Jun. 1997, pp. 1703–1708.

[27] P. P. Yip, J. K. Hedrick, and D. Swaroop, "The use of linear filtering to simplify integrator backstepping control of nonlinear systems," in *Proc. IEEE Int. Workshop Variable Struct. Syst. (VSS)*, Dec. 1996, pp. 211–215.
[28] J. A. Farrell, M. Polycarpou, M. Sharma, and W. Dong, "Command filtered backstepping," *IEEE Trans. Autom. Control*, vol. 54, no. 6, pp. 1391–1395, Jun. 2009.
[29] M. Sharma and A. J. Calise, "Adaptive backstepping control for a class of nonlinear systems via multilayered neural networks," in *Proc. Amer. Control Conf.*, May 2002, pp. 2683–2688.
[30] D.-H. Shin and Y. Kim, "Reconfigurable flight control system design using adaptive neural networks," *IEEE Trans. Control Syst. Technol.*, vol. 12, no. 1, pp. 87–100, Jan. 2004.
[31] C. P. Bechlioulis and G. A. Rovithakis, "A low-complexity global approximation-free control scheme with prescribed performance for unknown pure feedback systems," *Automatica*, vol. 50, no. 4, pp. 1217–1226, Apr. 2014.
[32] J. Q. Han, "Nonlinear tracking-differentiator," *J. Syst. Sci. Math. Sci.*, vol. 14, no. 2, p. 177, 1994.
[33] A. Levant, "Higher-order sliding modes, differentiation and output-feedback control," *Int. J. Control*, vol. 76, nos. 9–10, pp. 924–941, Jan. 2003.
[34] S. Huang, K. K. Tan, and T. H. Lee, "An improvement on stable adaptive control for a class of nonlinear systems," *IEEE Trans. Autom. Control*, vol. 49, no. 8, pp. 1398–1403, Aug. 2004.

JIAQI GU received the B.S. degree from Nanjing University of Science and Technology (NJUST), Nanjing, China, where he is currently pursuing the Ph.D. degree with the School of Energy and Power Engineering. His research interests include prescribed performance control and its application in unmanned systems.

RUISHENG SUN was born in 1978. He received the Ph.D. degree in navigation, guidance, and control from Nanjing University of Science and Technology (NJUST), China, in 2010. He is currently a Professor at NJUST. His research interests include nonlinear adaptive control and guidance, adaptive observer design, and multidiscipline optimization.

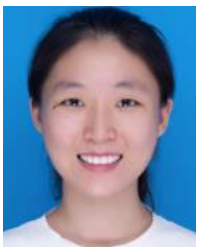

JIEQING CHEN received the B.S. degree in weapon launch engineering from Nanjing University of Science and Technology (NJUST), in 2018, where she is currently pursuing the Ph.D. degree with the School of Energy and Power Engineering. Her research interests include aircraft guidance, parameter estimation, system identification, adaptive control, and prescribed performance control.